International Journal of Heat and Mass Transfer 52 (2009) 5970–5977

Contents lists available at ScienceDirect

International Journal of Heat and Mass Transfer

journal homepage: www.elsevier.com/locate/ijhmt

Heat transfer and friction characteristics of solar air heater ducts having integral inclined discrete ribs on absorber plate

K.R. Aharwal [a,1], Bhupendra K. Gandhi [b,*], J.S. Saini [c,2]

[a] Mechanical Engineering Department, Shri G.S. Institute of Technology and Science, 23, Park Road, Indore, M.P. 452 003, India
[b] Department of Mechanical and Industrial Engineering, I.I.T. Roorkee, Roorkee, U.A. 247 667, India
[c] Deharadun Institute of Technology, Dehradun, U.A., India

ARTICLE INFO

Article history:
Received 20 September 2007
Received in revised form 12 March 2009
Accepted 22 May 2009
Available online 11 September 2009

Keywords:
Artificial roughness
Relative gap position
Relative gap width
Reynolds number
Nusselt number
Friction factor

ABSTRACT

The use of artificial roughness in a solar air heater duct has been proposed to be an excellent option to enhance the heat transfer from absorber plate to the air. This paper presents an experimental investigation on heat transfer and friction characteristics of solar air heater ducts with integral repeated discrete square ribs on the absorber plate. The effect of geometrical parameters, especially, the gap width and gap position has been investigated. The roughened duct has a width to height ratio (W/H) of 5.83. The relative gap position (d/W) and relative gap width (g/e) has been varied from 0.16 to 0.5 and 0.5–2.0, respectively. Experiments have been carried out for the range of Reynolds number from 3000 to 18,000 with the relative roughness pitch (P/e) range of 4–10; relative roughness height (e/D) range of 0.018–0.037; and angle of attack (α) range of 30–90°. The optimum values of parameters for rib arrangement have been obtained and discussed. For Nusselt number, the maximum enhancement of the order of 2.83 times of the corresponding value of the smooth duct has been obtained, however, the friction factor has also been seen to increase by 3.60 times of that of the smooth duct. The maximum enhancement is observed at a relative gap position of 0.25 for relative gap width of 1.0, relative roughness pitch of 8.0, angle of attack of 60° and relative roughness height of 0.037. Based on the experimental data, correlations for Nusselt number and friction factor have been developed as function of roughness parameters of inclined discrete square ribs and flow Reynolds number.

1. Introduction

Thermal performance of a conventional solar air heater has been observed to be poor because of the low value of convective heat transfer coefficient between the absorber plate and the working fluid even for turbulent flow. It was reported that the thermal resistance for the convective heat transfer is mainly caused by the viscous sub-layer developed at the heat-transferring surface. Therefore, efforts have been generally made to destroy or break this sub-layer. The use of artificial roughness, in addition to enhancing heat transfer coefficient considerably, results in higher frictional losses leading to the excessive power requirement for flow of the working fluid (air) through the duct. It is therefore essential to optimize the geometrical parameters of the artificial roughness in order to achieve the maximum possible gain in heat transfer with minimum penalty in terms of increased frictional losses.

Analytical methods for predicting the heat transfer coefficient (or Nusselt number) and friction factor in channels with various types of roughness geometries are not available, as a complete understanding of turbulent flow is still lacking. The flow structure over the roughened surface is quite complex and depends on the angle of attack, duct aspect ratio, rib shape and rib height to pitch ratio. Attempts have been made by many investigators [5–10] to develop correlations based on the rib configuration and flow Reynolds number for predicting the heat transfer coefficient and friction factor using two different techniques. In one technique, the investigators have developed semi-empirical correlations for heat transfer and friction factor in terms of heat transfer function G and roughness function $Re\ (e^+)$, respectively, and in the second technique, semi-empirical correlations for heat transfer coefficient and friction factor have been developed in terms of Nusselt number and friction factor, respectively. Nikuradse [1] was probably the first one to develop the friction similarity law for the sand–grain roughened surface as follows:

$$u^+ = 2.5\ln(y/e) + R(e^+) \tag{1}$$

where u^+ is dimensionless velocity (m/s), y is distance from the wall (m), e is rib height (m), and $R(e^+)$ momentum transfer roughness function.

* Corresponding author. Tel.: +91 9412920113; fax: +91 1332 285665.
E-mail addresses: kraharwal@yahoo.com (K.R. Aharwal), bkgmefme@iitr.ernet.in (B.K. Gandhi), sainifme@iitr.ernet.in (J.S. Saini).
1 Tel.: +91 9406668576; fax: +91 1332 285665.
2 Tel.: +91 9411151702; fax: +91 1332 285665.

0017-9310/$ - see front matter © 2009 Published by Elsevier Ltd.
doi:10.1016/j.ijheatmasstransfer.2009.05.032

The momentum transfer roughness function $R(e^+)$ attains a constant value in fully rough flow condition for a given roughness geometry and its value is different for different roughness geometry conditions.

Webb et al. [2] extended the law of wall and the heat momentum transfer analogy to geometrically non-similar roughness and developed friction factor correlations for flow in circular tubes with transverse ribs for fully rough flow regions ($e^+ > 35$). These correlations have been used by Han et al. [3] for different rib roughness geometries who reported that it is difficult to develop a universal correlation for different types of roughness geometries. Dipprey and Sabersky [4] developed heat and momentum transfer analogy for flow in tubes having sand grain roughness which is expressed as under,

$$G(e^+, P_r) = [(f/2S_t) - 1](f/2)^{-0.5} + R(e^+) \tag{2}$$

where e^+ is roughness Reynolds number; G is heat transfer function; f is friction factor; P_r is Prandtl number and S_t is Stanton number.

It should be emphasized that the heat transfer function, G (Eq. (2)) depends on the specified type of geometrically similar roughness. Therefore, this analogy may not be extensively used for computation of heat transfer coefficient for the flow through all kinds of rough surfaces.

Prasad and Saini [5] proposed semi-empirical correlations, based on the law of wall similarity, for heat transfer coefficient and friction factor of a solar air heater having the artificially roughened absorber plate which are expressed as under,

$$\overline{St} = \frac{\bar{f}/2}{1 + \sqrt{\left(\bar{f}/2\right)}\left[4.5(e^+)^{0.28}\mathrm{Pr}^{0.57} - 0.95(P/e)^{0.53}\right]} \tag{3}$$

The average friction factor $\bar{f}$ of solar air heater duct is given by

$$\bar{f} = \frac{(W + 2B)f_s + Wf_r}{2(W + B)} \tag{4}$$

and friction factor for roughened duct, f_r is given by,

$$f_r = \frac{2}{\left[0.95(P/e)^{0.53} + 2.5\ln(D/2e) - 3.75\right]^2} \tag{5}$$

where $\overline{St}$ is average Stanton number, P/e is the relative roughness pitch, W is the width of the duct (m), B is the depth of the duct (m), D is the hydraulic diameter of the duct (m), e is the roughness height (m) and f_s is the friction factor for smooth duct.

Gupta et al. [6] used inclined rib configuration for enhancement of heat transfer of solar air heater and developed correlations for heat transfer coefficient and friction factor. Karwa et al. [7] used chamfered rib arrangement for enhancement of thermal performance of solar air heater and developed correlations for heat transfer coefficient and friction factor in terms of heat transfer function (G) and roughness function (R). Bhagoria et al. [8] used wedge shaped rib configuration for the enhancement of heat transfer of solar air heater and developed correlations for heat transfer coefficient and friction factor in terms of Nusselt number and friction factor. Similarly, Momin et al. [9] and Jaurker et al. [10] have employed artificial rib roughness in the form of V-shaped rib and rib-groove, respectively, to enhance the thermal performance of solar air heaters and developed the correlations for Nusselt number and friction factor. Cho et al. [11] investigated the effect of a gap in the inclined ribs on heat transfer in a square duct and reported that a gap in the inclined rib accelerates the flow and enhances the local turbulence which will result in an increase in the heat transfer. They reported that the inclined rib arrangement with a downstream gap position shows higher enhancement in heat transfer compared to that of the upstream gap rib arrangements. They, however, have not attempted to optimize the gap width and gap position. The task of optimization of the gap position and gap width for inclined ribs on the absorber plate of the solar air heater is undertaken in this work.

In this work, experimental investigations have been carried out on a rectangular duct having the absorber plate with artificial roughness in the form of inclined rib with a gap, to evaluate the enhancement in heat transfer coefficient and friction factor and consequently the thermo-hydraulic performance of the roughened ducts. The optimum values of parameters for rib arrangement have been obtained and discussed. Based on the experimental data, correlations for Nusselt number and friction factor have been developed as function of roughness parameters of inclined discrete ribs and flow Reynolds number. The roughness has been produced only on the underside of the top plate of the duct to simulate the conditions that prevail in a solar air heater where only top heated plate transfers the heat to the air from the under side only.

2. Experimental program and roughness geometry

An experimental test facility has been designed and fabricated to study the effect of a gap in the inclined rib on the heat transfer and friction characteristics of a rib-roughened rectangular duct. A schematic diagram of the experimental set up is shown in Fig. 1. The wooden rectangular duct has an internal size of 2600 mm × 181 mm × 31 mm which consists of entrance section, test section and exit section of lengths of 800 mm, 1200 mm and 600 mm, respectively, according to the guidelines of ASHARAE standard [12]. A 6 mm thick aluminum plate, roughened artificially at the wetted side, is used as the top broad wall of the test section whereas the upper walls of entry and exit sections of the duct were made of 12 mm thick plywood. The absorber plate is heated from the top by supplying a constant heat flux through an electrical heater, which was insulated by 50 mm thick glass wool and 12 mm thick plywood. A calibrated orifice-meter is used to measure the mass flow rate of air by measuring the pressure drop through a U-tube manometer with kerosene as manometric fluid. A Betz micro-manometer is used to measure the pressure drop across the test section. Calibrated thermocouples have been used for monitoring the temperature variations. The airflow rate has been varied with the help of a control valve to conduct the test in the flow Reynolds number range of 3000–18,000. Data are collected for steady-state condition only, which is assumed to have been reached when the plate and the air temperatures do not show any significant variation for 10-min duration.

Fig. 2(a)–(e) shows the roughness geometries employed. The absorber plates were machined to develop integral ribs on the surface of an Aluminum plate. The height of the rib is varied from 1 mm to 2 mm whereas its width is kept equal to 2 mm. The effect of a gap in the ribs on the absorber plate of solar air heater has been investigated. The relative gap position (d/W), defined as the ratio of gap position from trailing edge (projected along the width) to duct width, is varied from 0.167 to 0.67 and relative gap width (g/e), defined as the ratio of gap width to rib height, is varied from 0.5 to 2.0. The relative roughness height (e/D), defined as rib height to hydraulic diameter of the duct, is varied from 0.018 to 0.037.

3. Data reduction

Steady state values of the plate and air temperatures at various locations were measured for a given heat flux and mass flow rate of air. The mass flow rate across the duct is measured by measuring the pressure drop across a calibrated orifice-meter through a U-tube manometer. In order to calculate the friction factor, the pressure drop across the test section has been measured by using a Betz micro-manometer. The following procedure has been em-

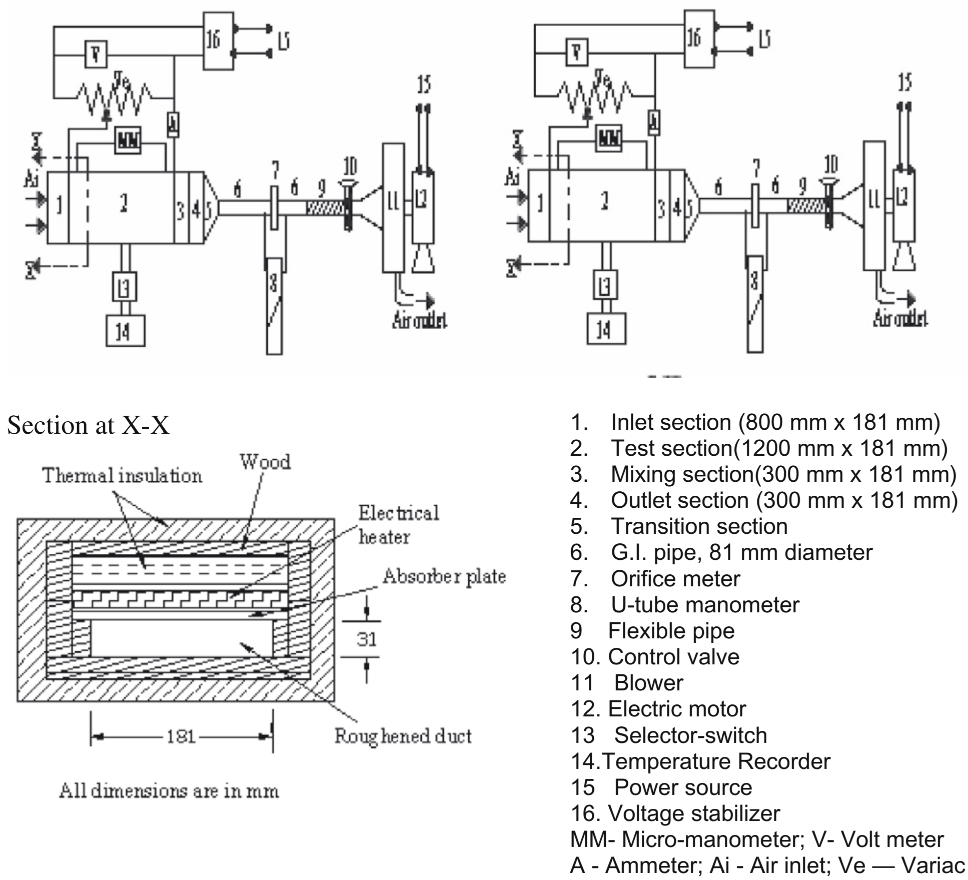

Fig. 1. Schematic diagram of experimental set-up.

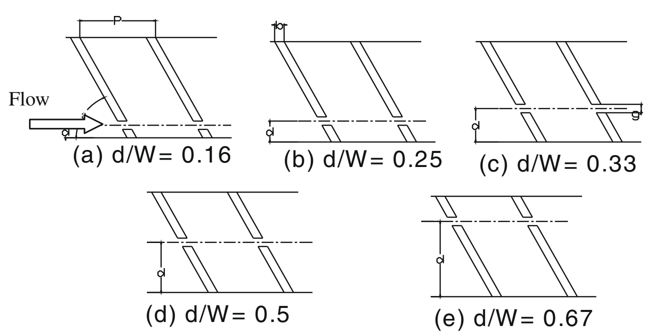

Fig. 2. Rib roughness geometry.

ployed for the calculation of heat transfer coefficient 'h', Nusselt number 'Nu', Reynolds number 'Re' and friction factor 'f'.

The heat transfer coefficient for the heated section was calculated from the equation given below,

$$h = \frac{Q_u}{A_p \cdot (T_p - T_f)} \tag{6}$$

where A_p is the area of the absorber plate (m^2), T_p is the average plate temperature (K) and T_f is the average of the inlet and outlet temperatures of the air (K).

The rate of heat gain by the air 'Q_u' is given by,

$$Q_u = mC_p(T_0 - T_i) \tag{7}$$

where C_p is the specific heat capacity (J/kg K), and T_i and T_0 are inlet and outlet temperature of the air, respectively (K).

Mass flow rate 'm', has been determined from the pressure drop measurement across the orifice-meter.

$$m = C_d A_0 \left[2\rho(\Delta P)_0/\left(1-\beta^4\right)\right]^{0.5} \tag{8}$$

where A_0 is cross-section area of orifice (m^2), C_d is the discharge coefficient of the orifice (determined as 0.6013 through calibration); $(\Delta P)_0$ is the pressure drop across the orifice-meter (Pa), β is the ratio of orifice diameter to pipe diameter and ρ is the density of air (kg/m^3).

Heat transfer coefficient is used to determine the Nusselt number using the equation,

$$Nu = \frac{h \cdot D}{k} \tag{9}$$

where h is the convective heat transfer coefficient (W/m^2 K), k is thermal conductivity of air (W/m K).

The friction factor (f) is determined from the flow velocity 'V' and the pressure drop '$(\Delta P)_d$' measured along the test section for a length of 1.0 m and applying Darcy–Weisbach equation as,

$$f = \frac{2 \cdot (\Delta P)_d \cdot D}{4 \cdot \rho \cdot L \cdot V^2} \tag{10}$$

where L is length of test section (m), $(\Delta P)_d$ is pressure drop in the test section (Pa) and V is velocity of fluid inside the duct (m/s).

Based on the analysis of the errors in the experimental measurements using different instruments, the uncertainties in the calculated values of Reynolds number, Nusselt number, and friction factor have been estimated as ±2.6%, ±2.3% and ±7.5%, respectively, at Reynolds number of 3000 and as ±1.8%, ±3.1% and ±3.5%, respectively, at Reynolds number of 18,000 [13].

4. Validation of experimental data

The Nusselt number and friction factor evaluated from experimental data for smooth duct have been compared with the values obtained from Dittus–Boelter equation and modified Blasius equation for Nusselt number and friction factor, respectively [14].

The Nusselt number for a smooth rectangular duct (Nu_s) is given by Dittus–Boelter equation as,

$$Nu_s = 0.023Re^{0.8}P_r^{0.4} \tag{11}$$

The friction factor for a smooth rectangular duct (f_s) is given by modified Blasius equation as,

$$f_s = 0.085Re^{-0.25} \tag{12}$$

Eqs. (11) and (12) have been used to estimate Nusselt number and friction factor at different Reynolds numbers and the estimated values are compared with the experimentally measured values. It is observed that the average deviations between the two values are ±2.8%, and ±2.3% for Nusselt number and friction factor, respectively [15]. This shows reasonably good agreement between the two values for the Reynolds number for the range of this investigation, which ensures the accuracy of the data being collected with the experimental setup.

5. Results and discussion

The values of Nusselt number, friction factor and thermo-hydraulic performance parameter of the roughened duct as function of roughness parameters and Reynolds numbers have been plotted in Figs. 3–12. Fig. 3(a) shows the effect of relative gap position (d/W) on Nusselt number for a fixed value of relative roughness pitch (P/e) of 8.0, angle of attack of 60°, relative roughness height of 0.037 and relative gap width (g/e) of 1.0. It is seen that for any Reynolds number, the value of Nusselt number is higher for a gap in the continuous rib as compared to that of the rib without gap and that the Nusselt number increases with increase in the relative gap position from 0.16 to 0.25, attains the maximum value at a gap position of 0.25 and thereafter it decreases with an increase in the relative gap position. The enhancement of heat transfer coefficient based on Nusselt number ratios lies in the range of

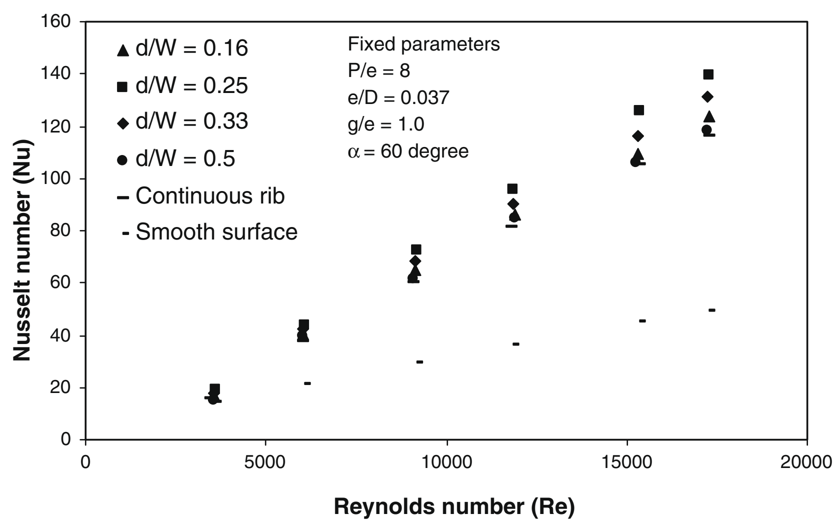

Fig. 3(a). Variation of Nusselt number with Reynolds number as a function of relative gap position.

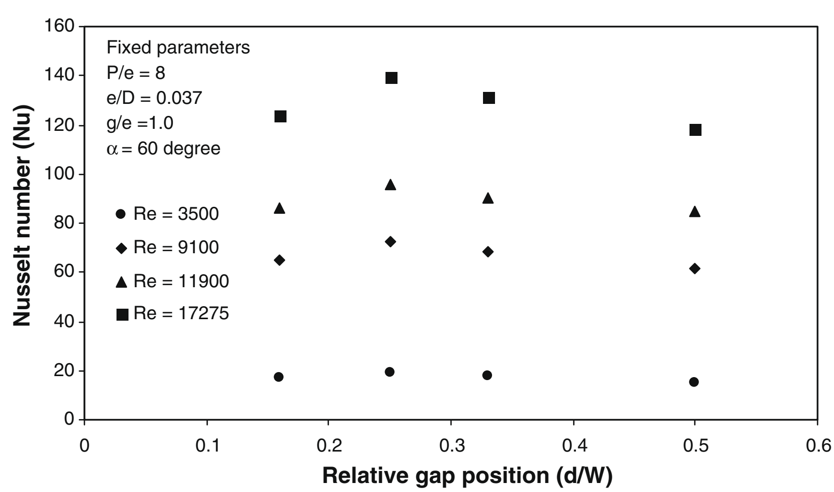

Fig. 3(b). Variation of Nusselt number with relative gap position at few selected Reynolds numbers.

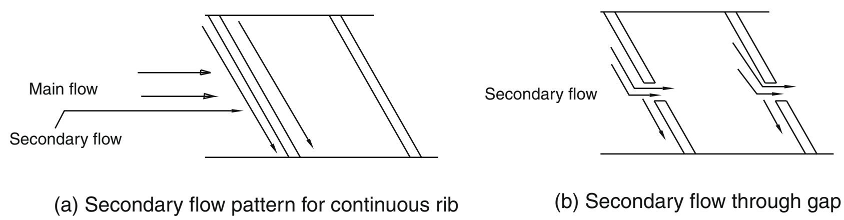

Fig. 4. Flow pattern of secondary flow.

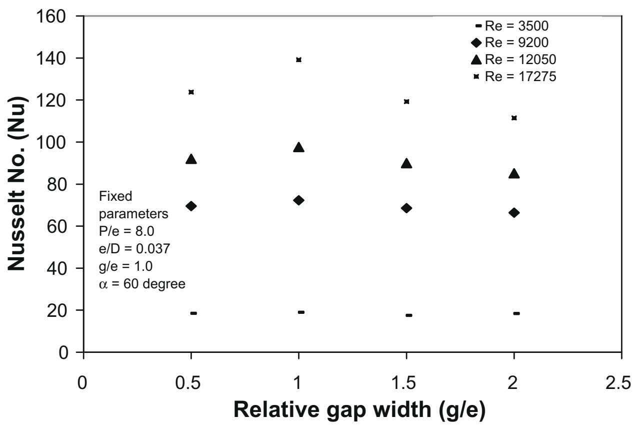

Fig. 5. Variation of Nusselt number with relative gap width (g/e) at few selected Reynolds numbers.

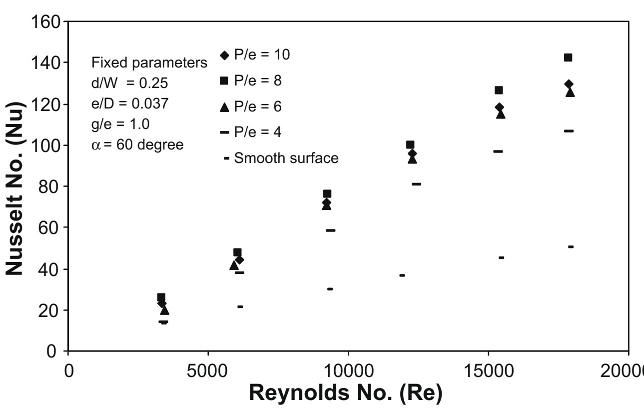

Fig. 6. Variation of Nusselt number with Reynolds number at different relative roughness pitches (P/e).

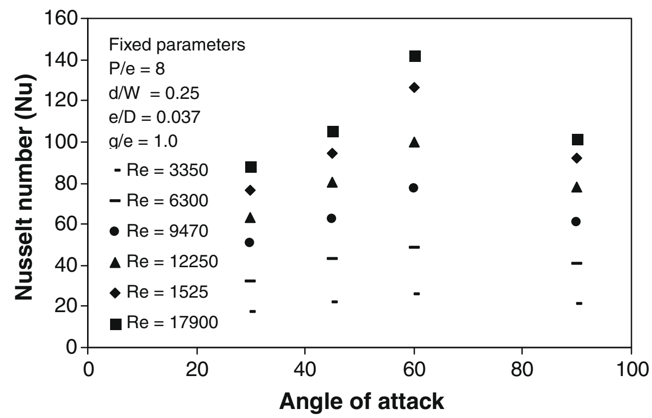

Fig. 7. Nusselt number variation as a function of angle of attack (α) at few selected Reynolds numbers.

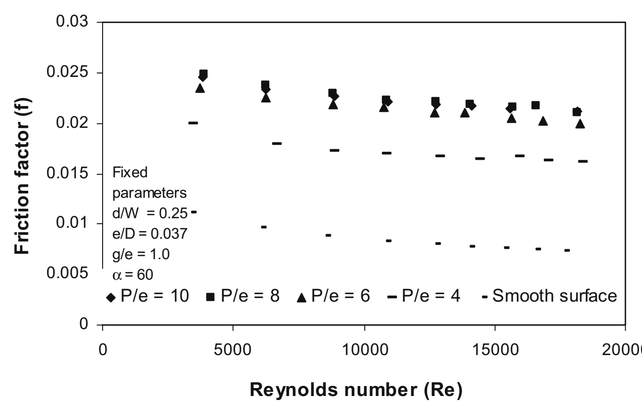

Fig. 8. Variation of friction factor with Reynolds number at different relative roughness pitch (P/e) values.

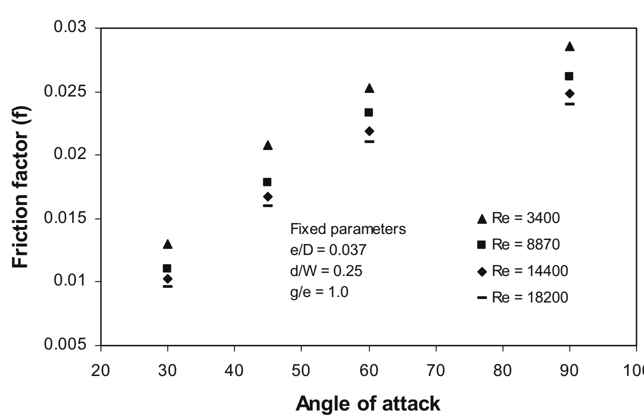

Fig. 9. Variation of friction factor with angle of attack (α) at selected Reynolds numbers.

1.53 times to 2.83 times of that of the smooth surface duct under similar operating conditions.

In order to bring out the effect of gap position clearly, the variation of Nusselt number with relative gap position is presented in Fig. 3(b) at few selected Reynolds number values where clear maxima at relative gap position of 0.25 can be observed. This is explained by the flow phenomenon as discussed below.

An inclined rib in a rectangular duct gives rise to secondary flow along the rib length, which allows the working fluid to travel from leading edge to trailing edge of the rib as shown in Fig. 4(a). The fluid flowing along the rib is gradually heated and boundary layer grows thicker [16]. Introduction of a gap in the rib allows release of fluid belonging to secondary flow and main flow through the gap as shown in Fig. 4(b). The main flow passing through the gap is the developed flow with thicker boundary layer consisting of viscous sub-layer. As a result of the presence of gap, the secondary

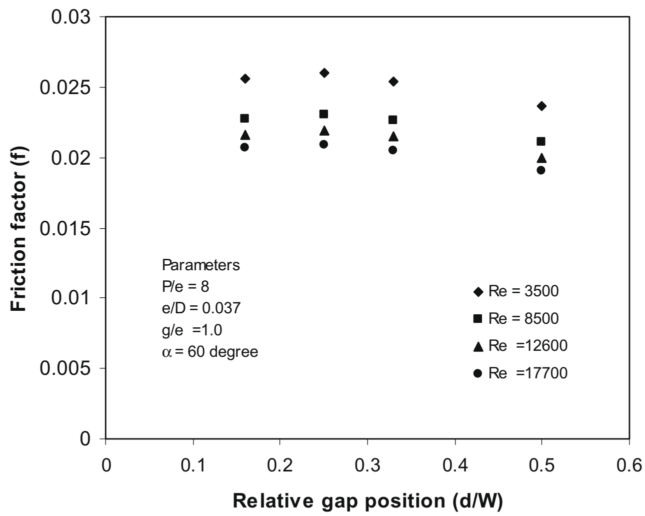

Fig 10. Variation of friction factor with relative gap position (d/W) at few selected Reynolds numbers.

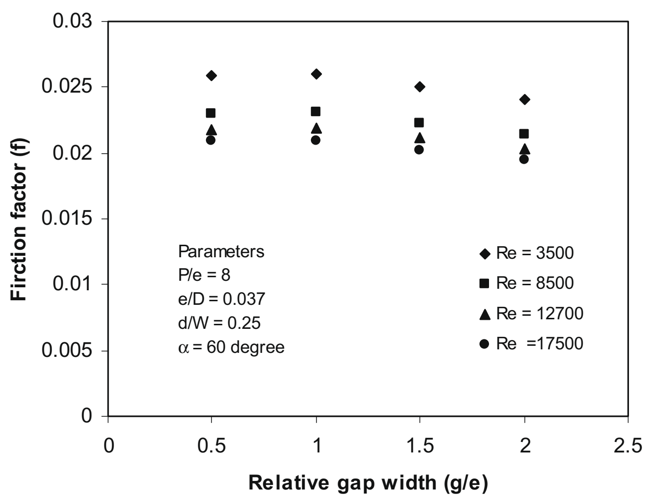

Fig 11. Variation of friction factor with relative gap width (g/e) at few selected Reynolds numbers.

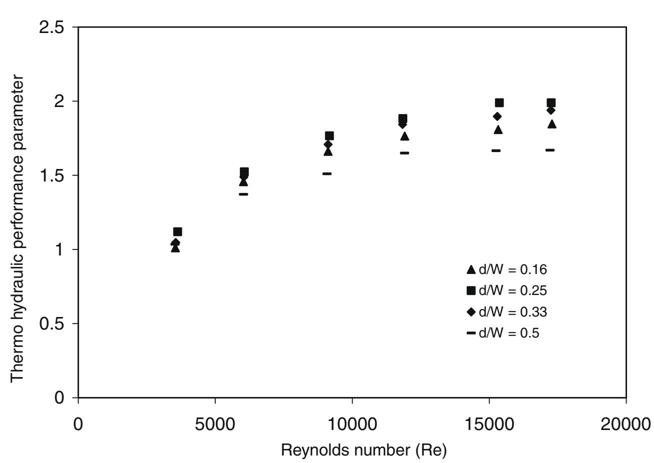

Fig. 12. Thermo-hydraulic performance for different roughness geometries.

flow along the rib joins the main flow to accelerate it which energizes the retarded boundary layer flow along the surface. This increases the heat transfer through the gap width area behind the rib. It is to be pointed out that the inclination of rib creates a high heat transfer region at the leading edge and a low heat transfer region at the trailing edge. If the gap is created towards the trailing edge region, this helps in eliminating the low heat transfer trailing edge region and hence overall heat transfer is enhanced. This is seen to happen till the gap position is about one fourth of the duct width, possibly because placing a gap at a position too close to the duct wall is not likely to produce similar effect of enhancement due to the presence of lateral boundary layer near to the wall and hence further decrease of gap position, i.e. placing the gap closer to the trailing edge ($d/W < 0.25$) results in a decrease in the overall heat transfer rate. Cho et al. [11] have also reported that a gap at the leading edge side of the inclined rib reduces the heat transfer compared to that at the trailing edge side. Thus it appears that at relative gap position of 0.25, the contribution of secondary flow in energizing the main flow through the gap results in the maximum value of heat transfer coefficient at any Reynolds number.

The effect of relative gap width (g/e) on Nusselt number is shown in Fig. 5 at few selected Reynolds numbers. It is seen that Nusselt number increases with an increase in the relative gap width up to about 1.0, beyond which it decreases with increase in the relative gap width. The value of Nusselt number is the maximum for the relative gap width of 1.0 and the minimum for the relative gap width of 2.0 for the range of investigation. The basic reason of creating a gap in the inclined rib is that, the gap flow promotes local turbulence and flow mixing along the gap flow region, while the rib-induced secondary flow is maintained in the duct [11]. Therefore, it may be reasoned that the increase in relative gap width beyond 1.0 reduces the flow velocities through the gap and hence the local turbulence. At the same time too small gap width will also not allow sufficient amount of secondary flow fluid to pass through and hence the turbulence level will remain low.

The variation of Nusselt number with Reynolds number as a function of relative roughness pitch for a relative gap position (d/W) of 0.25 and relative gap width of 1.0 is shown in Fig. 6. The maximum values of Nusselt number are observed to correspond to the relative roughness pitch of 8.0 and are of the order of 2.83 times of that of the smooth surface. As pointed out by Han and Park [17], the occurrence of the maximum value of Nusselt number at a certain relative pitch value signifies the presence of the reattachment point at an optimum position. As the relative roughness pitch is reduced to the value below 8.0, the flow is not likely to reattach before it reaches the successive rib. Therefore, the thermal performance of the duct deteriorates with decrease in the relative roughness pitch value below 8.0. On the other hand, an increase of the relative roughness pitch above 8.0, the number of reattachment points per unit length will reduce as compared to those with the relative roughness pitch of 8.0. This will reduce the amount of heat transfer and hence the Nusselt number is lower for the relative roughness pitch value higher than 8.0. Han et al. [3] have also reported that the rib configuration with relative roughness pitch of 7.5 gives higher enhancement in heat transfer than that of the relative roughness pitch of 10 or 5. Webb et al. [2] have reported that the maximum heat transfer occurred at a value of relative roughness pitch range of 6–8.

Fig. 7 shows the variations of Nusselt number as a function of angle of attack for selected values of Reynolds numbers. It is seen that the value of Nusselt number increases with increase in angle from 30° to 60°, attaining the maximum value at the angle of attack of 60° and then decreases with further increase in the value of angle of attack.

The variation of friction factor with Reynolds number for different values of relative roughness pitch is shown in Fig. 8 for the relative gap position (d/W) of 0.25, relative gap width (g/e) of 1.0, angle of attack of 90° and relative roughness height of 0.037. It is seen that the friction factor increases with increase in the relative roughness pitch from 4.0 to 8.0, attains the maximum value at the pitch of 8.0 and then decreases with further increase in the relative roughness pitch.

Figs. 9–11 present the effect of angle of attack, relative gap position and relative gap width, respectively, on friction factor at few selected Reynolds numbers. As shown in Fig. 9, the maximum value of friction factor is seen to correspond to an angle of attack of 90°, relative gap position of 0.25 and relative gap width of 1.0. Lau et al. [18] have reported that the value of friction factor for 90° discrete rib arrangements is higher than that of the 60°, 45° and 30° discrete rib arrangements. A relative gap position of 0.25 with the relative gap width of 1.0 appears to result in the maximum value of friction factor, however, the variation of friction factor with relative gap position or gap width is not very significant at any Reynolds number (Figs. 10 and 11).

5.1. Thermo-hydraulic performance

A parameter known as thermo-hydraulic performance parameter 'η' is used to evaluate the effectiveness of artificially roughened surfaces accounting for the enhancement of Nusselt number and friction factor and is expressed as $(Nu/Nu_s)/(f/f_s)^{1/3}$ [19]. Fig. 12 shows a plot of this parameter as a function of Reynolds number for some of the roughness geometries. It is seen that the inclined ribs with a gap gives higher thermo-hydraulic performance compared to that of the continuous rib arrangement for the entire range of Reynolds number. The value of this parameter is seen to increase with increase in the relative gap position up to 0.25 and decreases with further increase in the relative gap position at all values of the Reynolds number.

5.2. Correlations for Nusselt number and friction factor

As mentioned above, the analytical methods for prediction of heat transfer coefficient and friction factor in ducts with artificially roughened walls are not available, hence empirical correlations based on experimental data over the range of rib configuration and flow parameters have been developed. Results and discussion presented above reveal that Nusselt number of inclined rib-roughened geometry is a strong function of gap parameters namely, relative gap position (d/W) and relative gap width (g/e) at any Reynolds number as compared to the friction factor and the maximum values of Nusselt number and friction factor have been observed for relative rough pitch of 8 and angle of attack of 60°. Since most of experiments have been carried out at these optimum relative roughness pitch and angle of attach of the rib to investigate the effect of gap parameters, the correlations for Nusselt number and friction factor have also been developed for these conditions. Consequently, the functional relationship for Nusselt number and friction factor for these conditions can be written as:

$$Nu = Nu(Re, d/W, g/e \text{ and } e/D) \tag{13}$$

$$f = f(Re, d/W, g/e \text{ and } e/D) \tag{14}$$

5.2.1. Correlation for Nusselt number

A correlation has been developed by regression analysis of the experimental data obtained in this work. In order to find the functional relationship between Nusselt number and Reynolds number, a set of corresponding data points have been plotted on log–log scale. The functional relationship for Nusselt number and Reynolds number for all the data is given as:

$$N_u = A_0(Re)^{1.148} \tag{15}$$

Here the coefficient parameter, A_0 is a function of other affecting parameters like P/e, d/W, g/e, α and e/D.

In order to develop a relationship between A_0 and relative roughness height (i.e. e/D), the values of A_0 (= $Nu/Re^{1.148}$) are plotted against the values of e/D on log–log scale. Based on the nature of curve, the functional relationship of A_0 and the relative roughness height yields the equation.

$$\left[\frac{Nu}{Re^{1.148}}\right] = B_0\left(\frac{e}{D}\right)^{0.51}. \tag{16}$$

Here the value of B_0 is a function of other affecting parameters namely, relative gap position and relative gap width for a constant value of P/e and α. It has been shown that the maximum value of Nusselt number occurs at relative gap position of 0.25 and relative gap width of 1.0 which decrease with change in the value of any of the parameter (see Figs. 3 and 5). Further the effect of relative gap position was observed more dominating compared to the relative gap width. In order to develop a relationship between the parameter B_0 and relative gap position and relative gap width at value of P/e of 8 and α of 60°, the values of B_0 are plotted against a parameter which is the function of relative gap position and relative gap width which yields in the following relationship:

$$Nu = 0.0102Re^{1.148}(e/D)^{0.51}\left[\left\{1-\left(0.25-\frac{d}{W}\right)^2\left\{0.01\left(1-\frac{g}{e}\right)^2\right\}\right\}\right] \tag{17}$$

The above correlation (Eq. (17)) is developed for range of Reynolds number from 3000 to 18,000, relative roughness height from 0.018 to 0.037, relative gap position from 0 to 0.67 and relative gap width from 0 to 2.0 at relative roughness pitch of 8 and angle of attack of 60°.

5.2.2. Correlation for friction factor

A similar procedure has been employed to develop the correlation for friction factor. It was observed that the effect of a gap on the fiction factor is not very significant and therefore these parameters are not included in this correlation which is also applicable for the same range of parameters as Eq. (17). The final correlation for friction factor can be written in the following form:

$$f = 0.5Re^{-0.0836}(e/D)^{0.72} \tag{18}$$

The comparison between the experimental values of Nusselt number and friction factor and those predicted by the respective correlations, developed as Eqs. (17) and (18), respectively, has been carried out. It is observed that 99% of the data points of the Nusselt number lie within the deviation limits from +12% to −10%, and 99% of the data points of the friction factor lie within the deviation limits of ±10%.

6. Conclusions

Based on the experimental investigation on heat transfer and friction characteristics, it is found that as a result of providing gap in the inclined rib, there is considerable enhancement in heat transfer coefficient and friction factor of a rectangular artificially roughened duct with inclined and transverse discrete ribs on the absorber plate of solar air heater. The following conclusion can be drawn from this study:

1. As compared to the smooth surface, the rib-roughened surface yields an increase of about 2.83 and 3.60 times in the Nusselt number and friction factor, respectively, for the range of parameters investigated.

2. The maximum heat transfer enhancement occurs at the relative gap position of 0.25 with the relative gap width of 1.0 for the relative roughness pitch of 8.0, angle of attack of 60° and relative roughness height of 0.037.
3. The maximum value of friction factor occurs for discrete transverse ribs with relative roughness pitch of 8.0.
4. Correlations have been developed for Nusselt number and friction factor as function of roughness and flow parameters. These correlations have been found to predict the Nusselt number and friction factor values within deviation from +12% to −10% and ±10%, respectively, for the range of Reynolds number from 3000 to 18,000, relative roughness height from 0.018 to 0.037, relative gap position from 0 to 0.67 and relative gap width from 0 to 2.0 at relative roughness pitch of 8 and angle of attack of 60°.

References

[1] J. Nikuradse, Law of flow in rough pipes, in: National Advisory Committee for Aeronautics Technical Memorandum, 1950, p. 1292.
[2] R.L. Webb, E.R.G. Eckert, R.J. Goldstein, Heat transfer and friction in tubes with repeated rib roughness, Int. J. Heat Mass Transfer 14 (1971) 601–617.
[3] J.C. Han, L.R. Glicksman, W.M. Rosenow, An Investigation of heat transfer and friction for rib-roughened surfaces, Int. J. Heat Mass Transfer 21 (1978) 1143–1156.
[4] D.F. Dipprey, R.H. Sabersky, Heat and momentum transfer in smooth and rough tubes at various Prandtl numbers, Int. J. Heat Mass Transfer 6 (1963) 329–353.
[5] B.N. Prasad, J.S. Saini, Effect of artificial roughness on heat transfer and friction factor in a solar air heater: heat transfer characteristics of solar air heater, Sol. Energy 41 (6) (1988) 555–560.
[6] D. Gupta, S.C. Solanki, J.S. Saini, Heat and fluid flow in rectangular solar air heater ducts having transverse rib roughness on absorber plates, Sol. Energy 51 (1) (1993) 31–37.
[7] R. Karwa, S.C. Solanki, J.S. Saini, Heat transfer coefficient and friction factor correlation for the transitional flow regime in rib-roughened rectangular duct, Int. J. Heat Mass Transfer 42 (1999) 597–1615.
[8] J.L. Bhagoria, J.S. Saini, S.C. Solanki, Heat transfer coefficient and friction factor correlation for rectangular solar air heater duct having transverse wedge shaped rib roughness on the absorber plate, Renew. Energy 25 (2002) 341–369.
[9] A.M.E. Momin, J.S. Saini, S.C. Solanki, Heat transfer and friction in solar air heater duct with V-shaped rib roughness on absorber plate, Int. J. Heat Mass Transfer 45 (2002) 3383–3396.
[10] A.R. Jaurker, J.S. Saini, B.K. Gandhi, Heat transfer coefficient and friction characteristics of rectangular solar air heater duct using rib-grooved artificial roughness, Sol. Energy 80 (8) (2006) 895–907.
[11] H.H. Cho, Y.Y. Kim, D.H. Rhee, S.Y. Lee, S.J. Wu, The effect of gap position in discrete ribs on local heat/mass transfer in a square duct, J. Enhanced Heat Transfer 10 (3) (2003) 287–300.
[12] ASHARAE Standard 93-77 Methods of Testing to Determine the Thermal Performance of Solar Collectors, American Society for Heating, Refrigeration, and Air Conditioning Engineering, New York, 1997.
[13] J.P. Holman, Experimental Methods for Engineers, seventh ed., Tata McGraw-Hill, New Delhi, 2004.
[14] M.S. Bhatti, R.K. Shah, Turbulent and transition flow convective heat transfer, in: Handbook of Single-Phase Convective Heat Transfer, Wiley, New York, 1987.
[15] K.R. Aharwal, B.K. Gandhi, J.S. Saini, Experimental investigation on heat transfer enhancement due to a gap in an inclined continuous rib arrangement in a rectangular duct of solar air heater, Renew. Energy 33 (2008) 585–596.
[16] J.C. Han, W.L. Fu, L.M. Wright, Thermal performance of angled V-shaped and W-shaped rib turbulators in a rotating rectangular cooling channel, Trans. ASME J. Hear Transfer 126 (2005) 604–614.
[17] J.C. Han, J.S. Park, Developing heat transfer in rectangular channels with rib turbulators, Int. J. Heat Mass Transfer 31 (1) (1988) 183–195.
[18] S.C. Lau, R.D. McMillin, J.C. Han, Heat transfer characteristics of turbulent flow in a square channel with angled rib, Trans. ASME J. Turbomach. 113 (1991) 367–374.
[19] M.J. Lewis, Optimizing the thermo hydraulic performance of rough surface, Int. J. Heat Mass Transfer 18 (1975) 1243–1248.